

Conceptual Design of an Ion Microthruster**†

K. G. Hutchison
 S. B. Gabriel
 School of Engineering Sciences
 University of Southampton
 Southampton, Hants, SO17 3QX, UK
 +44 (0)2380 594876
 KGH@soton.ac.uk

IEPC-01-234

Abstract

The development of a viable micro ion thruster in the millinewton range, for use on nanosatellites in the mass range 1 to 10 kg, is a task presenting many problems. Primarily this is a result of the scaling laws of the physical parameters determining the performance of these devices. Some of the major problems faced are the sustenance of a magnetic field high enough to confine the electrons to ensure economic utilization and maintenance of a pressure in the chamber such that the electron mean free path is low enough to encourage efficient ionization. A theoretical model has been used to define the bulk properties of a Kaufman- type electrostatic ion thruster. The effect of each component's parameters on the overall thruster design was investigated and the equations presented classify a method of definitively describing a conceptual thruster from first principles. Assuming certain constraints can be satisfied, principally electron emission angle, magnetic field strength and ion extraction optics, it will be shown that the factors determining viability are compliance of a series of equations.

Key			
A_H	Hole Area, m^2	n_0	Neutral Number Density, atoms m^{-3}
d_1	Grid Separation, m	P	Pressure, Nm^{-2}
d_H	Hole Diameter, m	P'	Ionization Probability
I_b	Beam Current, A	Q	Volumetric Flow Rate, m^3s^{-1}
J_+	Max Current Density, Am^{-2}	R	Ideal Gas Constant
L_{CH}	Chamber Length, m	r_0	Beam Radius, m
l_h	Hole Length, m	r_H	Hole Radius, m
m	Mass Flow Rate, kgs^{-1}	T	Thrust, Nm^{-2}
m_{hole}	Mass Flow Rate per grid hole, kgs^{-1}	T_0	Temperature, K
m_i	Ion Mass, kg	u	Flow Velocity, ms^{-1}
N_A	Avogadro's Constant	V_{ex}	Exhaust Velocity, ms^{-1}
N_H	Number of Holes	V_p	Applied Potential, V
		V_{th}	Thermal Velocity, ms^{-1}
		x	Electron Path Length, m
		ϕ_0	Grid Transparency

* Presented as Paper IEPC-01-234 at the 27th International Electric Propulsion Conference, Pasadena, CA, 15-19 October, 2001.

† Copyright © 2001 Keith Hutchison. Published by the Electric Rocket Propulsion Society with permission.

γ	Electron Emission Angle, deg
η_u	Mass Utilization Efficiency
η_e	Electrical Efficiency
λ	Electron Mean Free Path, m
ρ	Density, kgm^{-3}
σ	Ionization Cross Section, m^2

Introduction

The brief of this project is to look at the relationship of size to physical aspects of a micro ion thruster. Under principal consideration are the hollow cathode device and the extraction electrodes. The scaling of ion thrusters and their components to low sizes is not well understood. The primary goal of this investigation is to look at the relationship between the practical operations of such devices and the theoretical understanding. On manufacture the thruster parts shall be individually performance tested then the device as a whole shall be analyzed and the degree of congruence between the results and theory shall be examined. The extent of these tests is limited to mass flow rate, pressure and current readings. Comparison with the code "PIC-DSMC" in development will allow further verification. Areas of specific interest include pressure variations and flow rates, which can be used to determine flows in the microchannels of the extraction grids, and the baffle geometries effect on electron flow.

Theory

Defining the requirements of the thruster allowed the design to be constructed around these factors.

PARAMETER	RANGE
Volume	1 – 10 cm^3
Thrust	0.5 – 1.5 $\times 10^{-3}$ N
Mass Utilization Efficiency	0.25 – 0.38 [1]
Electrical Efficiency	0.25 - 0.38
Mass Flow Rate	0.5 - 2 $\times 10^{-7}$ kgs^{-1}

Setting these allows other variables to be optimized although other influences, discussed later, must be taken into account.

As the thrust,

$$T = \eta_u . m . V_{ex}$$

the value of 40kms^{-1} for exhaust velocity V_{ex} lies in the requisite range.

$$V_{ex} = \sqrt{2eV_p/m_i}$$

therefore the applied extraction voltage is 1088.7 Volts[2]. This must be a primary calculation to permit grid design to prevent arcing. See section on Breakdown Potential. Setting the thrust and the exhaust velocity defines the beam current:

$$T = I_b \left(\frac{m_i}{e} \right) V_{ex}$$

According to the Child-Langmuir equation the maximum current density in the extraction grid region:

$$J_+ = \frac{4\epsilon_0}{9} \left(\frac{2e}{m_i} \right)^{1/2} \frac{V_p^{3/2}}{d_1^2} = \theta \frac{V_p^{3/2}}{d_1^2}$$

V_p is the applied potential

d_1 is the grid separation

θ , constant = $4.77\text{e-}9$ for $m_i = 2.1803\text{e-}25$ kg

As d_1 is set to 0.4mm, which must be well defined to determine the type of discharge occurring between the grids, and V_p is 1088.7 V then $J_+ = 1102.2 \text{ Am}^{-2}$. The total ion current able to penetrate the grids is the value of the Child-Langmuir maximum current density multiplied by the total extraction area, or $A_g \phi_0$. As the thruster is size limited a range of values is imposed on A_g . From our initial target parameters and their subsequent limiting of dependent factors, a value for ϕ_0 is evident. The grid transparency is defined by the equation:

$$\phi_0 = N_H \left(\frac{r_H}{r_0} \right)^2$$

Where N_H is the number of holes in the extraction grids, r_H is the radius of each hole and r_0 is the beam or chamber radius. For a defined transparency and beam diameter it is clear that $N_H \propto r_H^2$.

Pressure Balance

The internal pressure of the thruster must be balanced against several parameters affecting performance and optimized. Assuming the electrons are confined to orbits near the center of the chamber the length of this chamber is related to the ionization probability via:

$$P' = 1 - e^{(-x/\lambda)}$$

P' is the ionization probability, x is the path length the electron can subtend through the thruster, and λ is the mean free path (both in meters). To ensure efficient electrical operation $P > 0.5$, hence $x \geq 0.693\lambda$ x is dependent on the applied magnetic field:

$$\lambda = \frac{1}{n_0 \sigma}$$

n_0 is simply the number density of propellant atoms in the chamber and is dependent on pressure, while σ is the cross-section for ionization for the propellant gas, in this case for Xe it is $1.056 \times 10^{-21} \text{m}^2$.

$$n_0 = \frac{P \cdot N_A}{R \cdot T_0}$$

P is the pressure in Nm^{-2} , N_A is Avogadro's number, R is the ideal gas constant and T is the temperature in K.

Although the thruster is subject to a large pressure differential between the hot operating devices and the environment, the former will be well shielded and the total assembly large in comparison to these heat sources so temperature should be maintainable below 400K[3]. Higher pressures will reduce the path length increasing the probability of an ionizing collision. x is the maximum path length an electron can subtend through the thruster. As such lowering the angle of emission from the baffle is advantageous, as this angle will be maintained through the path as the electron spirals around the magnetic field. Assuming a helical

trajectory with no variation in angle of flight with respect to the thruster normal

$$x = \frac{L_{CH}}{\sin \gamma}$$

Where L_{CH} is the chamber length and γ is the angle of flight to thruster normal. A higher the pressure in the chamber means a shorter electron mean free path reducing the requirement for a low value of γ .

Pressure affects the breakdown potential between the extraction grids, the volumetric and mass flow rates from the chamber and the electrical efficiency of the thruster

Breakdown Potential

To prevent electrical arcing of the gas in diode configuration the Paschen curve illustrated below defines the discharge type, must be below the curve to prevent discharge. Therefore in our case the gas could inhabit both sides of Paschen curve, either $pd > 10 \text{kPa.cm}$ or $pd < 250 \text{ Pa.cm}$ although ascribing definitive values requires specific information on Xenon properties.

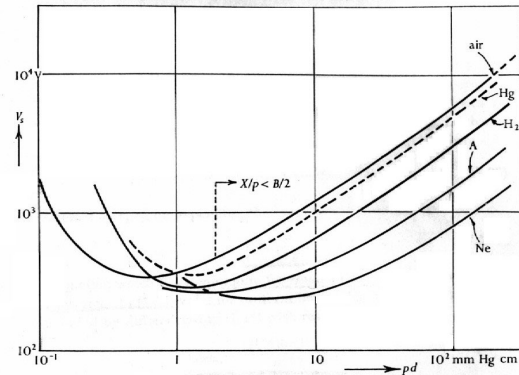


Fig 1 – Paschen Curves for Inert Gases [4]

Data for Argon (similar to Xe) shows that the minimum pressure multiplied by separating distance is equal to 80 mmHg cm at our accelerating potential of 1088.7 V, this is equal to 10664 Pa cm. At a grid separation of 0.4 mm a minimum average pressure of 250kPa must be maintained to inhibit electrical discharge if the area on the right side of the curve is to be inhabited. This means that the chamber pressure

must be greater still, up to twice this value, well beyond a practical value. If the left side of the curve is to be inhabited then the pressure must be small, in the region of less than 10Pa dictating a low chamber pressure although because this is not a parallel plate configuration it is postulated that the breakdown potential be somewhat modified by the electric field utilization factor for the extraction grid geometry allowing a higher effective pressure for this configuration. The following equations characterize sonic compressible choked flow :

$$u = \frac{Q}{A_H}, \quad m = \rho \cdot Q \quad \& \quad A_H = \frac{\pi}{4} d_h^2$$

$$\rho = \frac{P.W}{R.T_0} \quad \rho(\text{mean}) = \frac{(P_2 - P_1)W}{2.R.T_0}$$

$$u_{AVG} = (\eta_u \cdot V_{ex} + (1 - \eta_u) V_{th})$$

$$V_{th} = \sqrt{8kT_0 / \pi m_i}$$

In this case the ionic flow between the extraction grids is considered approximately the same as neutral flow, although much faster.

$$m = m_{hole} \cdot N_h$$

These equations allow flows to be determined from physical parameters measured from the system. Using the equation relating mass flow to open area [13]:

$$n_0 = \frac{4m(1 - \eta_u)}{m_i v_0 A_g \phi_0}$$

in this example the mass flow is measured in kgs^{-1} . This allows a relationship between mass flow rate and open area to be established.

Micro Ion Thruster Design

Consummate with the ideas of optimizing the efficiency of the micro ion thruster the parameters set

out in the theory above must be obeyed, which sets constraints on the design of certain parts of the system.

Miniature Hollow Cathode

The desired electron flux for our thruster is in the range of 100 mA, this is an order of magnitude greater than the beam current required to generate 500 μN of thrust, but as the current is controllable and electron losses are inevitable (to walls and cusps) a device with a more substantial range is desired. The format is the same as a conventional hollow cathode, only smaller [5,6]. See fig 2 below.

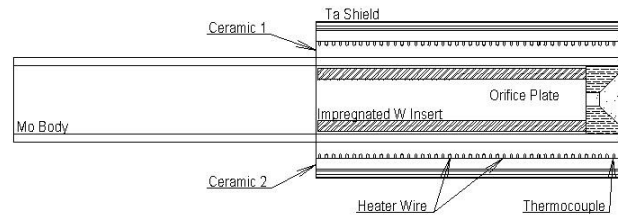


Fig 2 – Schematic of Hollow Cathode

The above sketch maps out the main hollow cathode parts, first the Molybdenum body acts as a gas feed and does expel a small number of electrons into the plasma acting as a source. The tungsten powder making up the insert is sintered to a level where at least 50% of the matrix is made up of free spaces between the particulates initially with liquid copper impregnated to facilitate the machining process. After the insert has been machined to the correct dimensions it is impregnated with BaCO_3 , CaCO_3 and Al_2O_3 at a ratio of 4:1:1 to a level where it makes up between 50% and 83% of the matrix. This mix is fed by capillary action into the pores of the sintered tungsten. After activation the oxides BaO and CaO form, which, under heating, will liberate electrons. The orifice plate is 2% thoriated tungsten; the thoria enhances thermionic electron emission. The active zone (plasma production volume) is situated around

the hole in the orifice plate and upstream (surrounded by insert)[7]. The orifice plate is chamfered to allow a good field of view upstream into the hollow cathode by the keeper electrode, not seen in this diagram [5,6].

The heater is wrapped around the cathode, as ignition of the electron flow generally requires a heat source. The heater is 0.1mm diameter 75% Tungsten, 25% Rhenium wire and is isolated from the body by a ceramic – Shapal-M. The Shapal-M is a non-toxic machinable ceramic with a high electrical resistance and a high thermal conductivity to allow the heat to freely permeate to the body, insert and orifice. This first ceramic has an isolated spiral groove into which the heater is placed as well as a further isolated horseshoe groove into which the Type K thermocouple is placed. Although temperatures exceed the narrow band values at which a type K is used, the expense is only a slight drop in sensitivity. At the projected temperature of 1200°C the error is less than 10°C. The second ceramic sheath, known as MACOR, is an electrical and thermal insulator to allow isolation of the heater and thermocouple, but to also provide maximum efficiency as the heat is being directed to the active area rather than away from it. Finally some dimpled tantalum foil is wrapped around the outer ceramic to give another layer of insulation, the dimpling reduces contact area increasing effective thermal resistivity. Once heated to around 1200K with a flow of neutral Xenon gas through equal to approximately 1×10^{-7} kgs⁻¹ a sustainable emission current should be reached in the region of hundreds of milliamps. This is significantly smaller than current devices in use and will provide an insight into the scaling relations of hollow cathodes. Note that the discharge voltage must be above the first ionization potential, but should be below the second ionization potential for the most efficient operation [8]

Baffle

The baffle serves to vector the electrons at a certain angle through the build-up of a space-charge layer, which then repels the incident electron beam creating a turbulent diffusive region just short of the baffle disc[9]. Electrons with the angle required (angle subtended between turbulent region and baffle annulus) will be ejected into the main ionization chamber spiraling down the magnetic field lines. The angle of the electrons leaving the baffle will be

maintained down the length of the thruster, dramatically increasing the electron path length, thereby increasing the efficiency of the device.

Chamber

The chamber is just a pocket where electrons from the hollow cathode may interact with the propellant gas ionizing it for acceleration through the extraction grid assembly.

Anode

The anode is a simple cylinder placed midway down the chamber and is present as a source to vector the electrons through an angle towards the downstream end of the thruster. It must not interfere in the line of sight between the baffle pole and the chamber pole. A potential below 50 Volts will be applied to this part of the device.

Extraction Electrodes

The extraction electrodes have proven a difficult matter to overcome in that the jobs they are perform are somewhat exclusive, and many factors play off against each other, so a comprehensive design for this part of the thruster system is required. First the two main tasks that the extraction electrodes must provide are (1) to accelerate ions to high velocities ($\sim 40\text{kms}^{-1}$) and (2) to provide an impedance to flow, maintaining a specified pressure in the ionization chamber. The greater the internal pressure the greater the propellant utilization efficiency. The grid design is to have a glass multichannel plate consisting of a sandwich of glass fibers running vertically from one side of the grid to the other, the center of each fiber will be removed leaving a multitude of holes through the sandwich which must be almost perfectly uniform to prevent impingement of the ion flow on the walls. Each side of the perforated glass plate will be coated with a metal; Molybdenum is a good candidate, to act as the electrodes.

Minimum Hole Size

Kaufman and Robinson state that as long as the proportions of hole diameters to each other and the proportions of the grid spacing to screen hole size are kept the same then “the current through a single hole is independent of either the absolute size of the hole or the grid spacing” [10]. Reduction in transmitted current in other experiments is most likely a result of poor grid alignment; microfabrication should solve alignment problems.

Plasma Surface at Acceleration Electrodes

Upon the generation of a plasma ions will drift towards region boundaries, reaching the edge of the plasma with a directed kinetic energy equal to $\sim kT_e$, falling through a sheath to the wall. Extraction of an ion beam generally requires that the wall have an aperture facing a well-aligned acceleration electrode through which the plasma may pass. The shape of the sheaths’ surface in the extraction hole region is dependent on the relation that the unipolar space charge problem inside the plasma boundary is approximately equal to the near zero field at the plasma surface taking account of the current density of slow ions delivered by the plasma. A concave plasma surface will focus the ions through the grid; a flat one will transmit ions in a uniform plane manner while a convex sheath will allow ions to spread in grid region, causing wall losses. It is obvious one of the former two cases is the desired set-up to minimize losses, increasing the potential difference between the grids or reducing the current density will allow formation of this concave surface.

Magnet Assembly

The magnets will take a ring-cusp configuration around the chamber and will be made of NdFeB, slightly less magnetic than the SmCo on offer, but with the ability to operate at higher temperatures. The magnets will be manufactured at the Rutherford Appleton Laboratory and will be layered on Kapton to allow easy mounting, in that they will simply be wrapped around the chamber. It is hoped that a field as high as 0.5 Tesla may be attained.

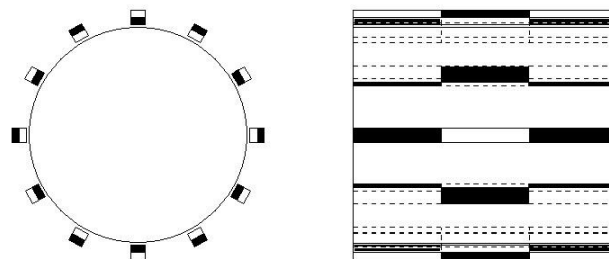


Fig 3 – Ring Cusp Magnet Configuration - different colours represent the different polarities

Neutralizer

In space conditions where grounding a device is not an option a charge-balance must be maintained to prevent the build-up of large amounts which in turn prevents destructive arcing. As this device may be open to vacuum an ideal candidate is a field emission array. Current technology shows that FEA’s may be operated at low pressures for hundreds of hours at emission currents of tens of micro amps, and as these are extremely small devices, typically $1/16\text{mm}^2$ then these can be expanded or connected to the thruster in numbers such that neutralization of charge resultant from ion acceleration is stable. The illustrations overleaf show the actual microtips and some associated failure modes. The central diagram shows a working tip, with a pronounced lip from the etching process, the diagram above this shows a tip which has been overdriven at high pressure and has partially vapourised establishing the unsuitability of these devices to use in the thruster ionization chamber, whilst the third diagram shows the loss of the anode as a result of excessive etching. This shows how the field emission arrays are very narrow band devices suited to neutralization in an ion thruster only.

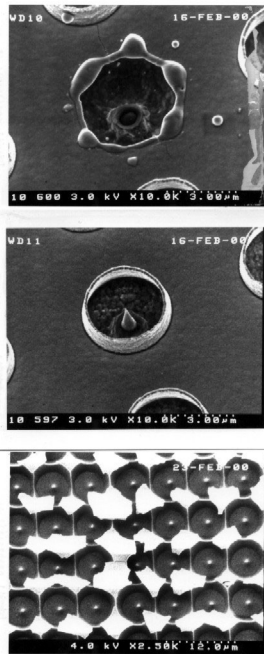


Fig 4 – SEM Photographs of FEA's

A neutralizer in the full flight configuration will eject an electron flux from the body of the thruster essentially equal to the ion beam flux to ensure that charge is balanced and no build-up of static charge on the spacecraft occurs, this variant is not really required in the laboratory configuration as grounding takes care of these charging effects. As the neutralizer will be open to space it can operate at lower pressures than the electron source in the thruster chamber, the required electron flux will be lower and the device power should be as low as possible.

$$P_{op} < 10^{-5} \text{ Nm}^{-2}$$

$$I_e = I_b$$

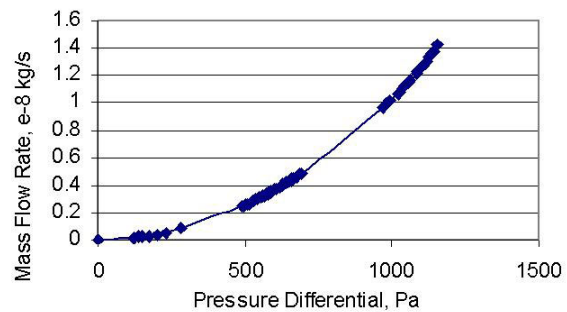
Field emission arrays are possible candidates for neutralizers on these thrusters; they are small, low power devices, which do not require some propellant and heating to initiate electron emission (as is the case with most hollow cathodes). The emission from these arrays is temperature insensitive between 130 & 360 K [11,12] so it is assumed that the current from such devices is invariant under the operating temperatures experienced in orbit (although this may drop considerably below 130K). The arrays themselves tested at RAL were capable of emission currents in the region of 30 to 80 μA per array (of 1600 tips).

Therefore approximately ten arrays would be required to act as a neutralizer for the thruster and the desired range of operating parameters it is intended to occupy.

The arrays of 1600 tips are in 40x40 tip rows over 0.25x0.25mm areas on wafers, a large array 10 times this size need only cover an area of $6.25\text{e-}7 \text{ m}^2$ or 0.8x0.8mm in a square array with the same tip dimensions. This size of array is easily compatible with mounting on the thruster body.

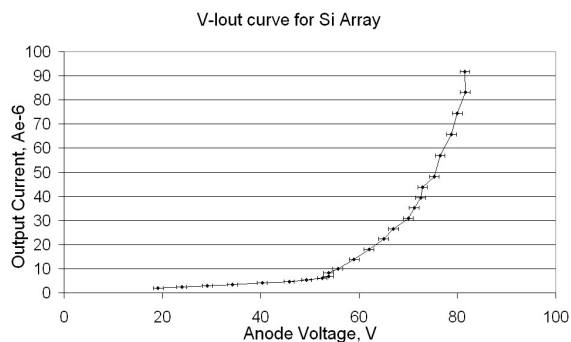
Results

The graph below shows the flow rates through a small capillary, though of a diameter and length greater than that seen in the extraction grids, with a smaller aspect ratio, it serves to illustrate the flow in the approximate region under investigation:



As can be seen the dependence of flow on pressure differential is non-linear and has a pressure squared relationship as expected. The flow was compressible in a choked condition. The capillary used here was of a length 11.15mm internal diameter 0.32mm, an aspect ratio of ~ 35 . The pressure differential and dimensions can be somewhat approximated to the case in the hollow cathode allowing for theoretical calculation of flows through this device to be made with confidence.

Theory states that the flow regime will be the same if the equations presented are adhered to.



The above graph relates the output current for a 0.25x0.25mm Silicon array of 1600 microtips operating at a pressure $\sim 10^{-5}$ Torr, which is sustainable in the space environment, demonstrating the applicability of these devices to neutralizer technology.

Verification from Code

In conjunction with the experimental investigation a colleague is developing a computer code able to predict results. The program is called "PIC-DSMC" standing for "Particle-in-Cell Direct Simulation Monte Carlo" which is a direct simulation plasma physics model. The code simulates rarefied gas dynamics and will be used for plume and chamber modeling as well as for micro/nano-fluidics. Current programs fail at Knudsen numbers greater than 0.1, this new code will work to Knudsen numbers of 2 and 3 comparable to microchannels in vacuum conditions.

Conclusions

On manufacture of the device a series of tests will show the degree of congruence between theoretical models of operation and actual efficiency of the thruster system. Preliminary flow tests have shown that the pressure differentials seen in the thruster should remain in the postulated regimes, which is not a requirement for operation, but is a requirement for the satisfaction of the theoretical model. The thruster will take the form of the schematic, fig 5, seen below with an additional field emission array neutralizer connected to the exterior.

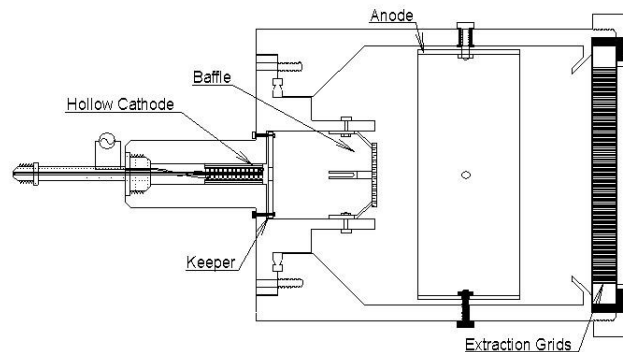


Fig 5 – Ion Thruster Schematic (surrounding magnet assembly not shown)

This is similar in every way to traditional designs except that it is smaller by a factor of 5 or more. This has its' greatest implications in operation of the hollow cathode and the extraction grids, testing of these two principal components will permit a greater understanding of the underlying physics and can be used as verification of the code "PIC-DSMC".

References

- [1] G Sandonato et al "Magnetic Confinement Studies for Performance Enhancement of a 5-cm Ion Thruster" IEEE Trans. on Plasma Science Vol 24 No 6 pp 1319-1329
- [2] G Yashko, Giffin "Design Considerations in Ion Microthrusters" IEPC 97-072
- [3] PJ Wilbur, JR Brophy "The Effect of Discharge Wall Temperature on Ion Thruster Performance", AIAA Jnl 24/2 pp 278-283
- [4] A. Von Engel "Ionized Gases" pp195
- [5] OA Gorshkov, VA Muravlev "An experimental investigation of the Hollow Cathodes for Low-Power Ion Thruster" IEPC-99-124 pp689-694
- [6] MT Domonkos "An Investigation into Orificed Hollow Cathodes" PhD Thesis,
- [7] A Salhi, PJ Turchi "Scaling Relations for Design & Operation of Orificed Hollow Cathodes" AIAA 94-3133
- [8] M J Patterson, S P Grisnik et al "Scaling of Ion Thrusters to Low Power" IEPC 97-098
- [9] A Malik "Role of Magnetic Field in Kaufman Type Electrostatic Ion Thrusters", IEPC 99-141 pp 767-773

- [10] HR Kaufman, RS Robinson “Minimum hole size in ion optics”, Journal of Spacecraft Vol 22 No 3 pp 381-382
- [11] B Kent, E Huq et al “The use of Microfabricated Field Emitter Arrays in a High Precision Mass Spectrometer for the Rosetta Mission”
- [12] S Meassick, H Champaign “The Effects of Fill Gases on the Failure Rate of Gated Silicon Field Emitter Arrays” pp207-210
- [13] J Brophy, P Wilbur “Calculation of Plasma Properties in Ion Sources” AIAA Jnl 24/9 pp1516 -1523